

Direct Measurement of the Longitudinal Coherence Length of a Thermal Neutron Beam

H. Kaiser, S. A. Werner, E. A. George^(a)

*Physics Department and Research Reactor Facility, University of Missouri-Columbia,
Columbia, Missouri 65211*

(Received 27 December 1982)

When a series of aluminum slabs are placed in one leg of a perfect-silicon-crystal neutron interferometer, a continuous and significant loss of contrast is observed. This observation is interpreted as being due to the finite length of the neutron wave packets.

PACS numbers: 03.65.Bz, 42.50.+q

A collimated beam of thermal neutrons prepared by Bragg reflection from a single crystal, or by passage through a pair of phased Fermi choppers, is never precisely monochromatic. According to the rules of quantum mechanics we are led to believe that we can describe a particular neutron in the beam by constructing a wave packet $\psi(x, t)$ from the linear superposition of plane waves $e^{i(kx - \omega t)}$ with amplitudes $a(k)$. The spatial extent σ_x of the wave packet is related to the width σ_k of the amplitude function $a(k)$ by the uncertainty principle:

$$\sigma_x \sigma_k \gtrsim \frac{1}{2}. \quad (1)$$

This alone does not tell us anything about the coherent internal structure of the wave packet or about its precise shape at a given instant of time. For a Gaussian amplitude function

$$a(k) = a_0 \exp[-(k - k_0)^2 / 4\sigma_k^2], \quad (2)$$

it is straightforward to show that the wave packet in real space also has a Gaussian shape with a width which increases with time, t , according to the formula¹

$$\sigma_x^2(t) = \frac{1}{4\sigma_k^2} + \frac{\hbar^2 t^2}{m^2} \sigma_k^2. \quad (3)$$

For a photon in vacuum this spreading does not occur, since the velocity of light is a constant, independent of k .

Are the coherent internal structure of the neutron wave packet, its shape, and this spreading with time accessible to experiment? Conceptually, at least, one might think so. Consider the following interferometric experiment, shown schematically in Fig. 1, in which we coherently split a neutron beam at point A , allow one of the beams to traverse a region of potential V extending over a distance D , and then allow it to recombine and interfere with the other beam at point B . The potential has the effect of increasing the transit time of the neutron wave packet of path I relative to the one on path II such that their mean

relative positions are displaced by a distance

$$\Delta x = \frac{1}{2} DV/E, \quad (4)$$

upon recombination near point B . In writing Eq. (4) we have assumed that the potential V is small in comparison to the kinetic energy E of the neutron. If the spatial shift Δx of the one wave packet with respect to the other is sufficiently large, they will no longer overlap near point B , and the contrast of the interferometer will disappear. By observing the change of contrast of the interferometer as a function of Δx , it is apparent that the shape and spatial extent of the neutron wave packet can be measured. More precisely, an experiment of this type is sensitive to the convolution of $\psi_I(x, t)$ with $\psi_{II}(x, t)$. The coherence length of an electron wave packet has recently been measured in a conceptually similar, but geometrically quite different, experiment with a Wien filter by Möllenstedt and Wohland.²

We have carried out this neutron experiment, utilizing a three-crystal silicon interferometer (Fig. 2) of the type developed by Bonse and Hart³ for x rays, and subsequently first shown to work for neutrons by Rauch, Treimer, and Bonse.⁴ This device has been used for a number of inter-

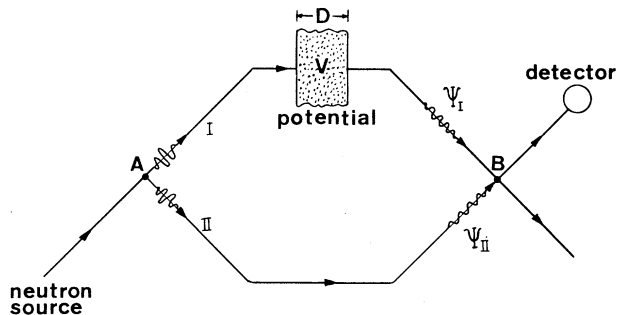


FIG. 1. Schematic diagram of an interferometer in which a nominally monoenergetic neutron beam is coherently split at point A and recombined at point B . The beam on path I traverses a region of positive potential V extending over a distance D .

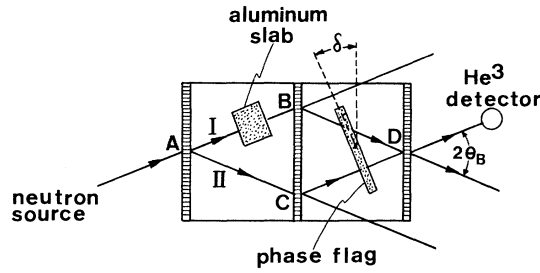


FIG. 2. Diagram of a Bense-Hart perfect-silicon-crystal interferometer. The collimated (0.7°) beam from a double-Cu(220)-crystal monochromator is split at point A and recombined at point D. The aluminum slab creates a positive potential and delays the neutron wave packet on leg I relative to leg II. The neutron wavelength $\lambda = 1.268 \text{ \AA}$, $d = 3.452 \text{ cm}$, $a = 2.464 \text{ cm}$, and $\theta_B = 19.3^\circ$.

esting neutron experiments in recent years.^{5,6}

If we place a slab of material, in this case made of polished, pure aluminum, in one leg of the interferometer, the wave packet traversing this path will be delayed relative to the wave packet traversing the other path as a result of the mean optical potential that it experiences in interacting with the aluminum nuclei. The optical potential, expressed in terms of the neutron-nucleus scattering length b ($= 3.5 \text{ fm}$ for Al) and the atom density N is^{7,8}

$$V = 2\pi\hbar^2 N b / m. \quad (5)$$

Combining this with Eq. (4), and writing the neutron's momentum in terms of its de Broglie wavelength λ , we see that the spatial shift is

$$\Delta x = -\lambda^2 D b N / 2\pi. \quad (6)$$

For the 1.268-\AA neutrons used in our experiment, this yields $\Delta x = 54 \text{ \AA}$ for a 1-cm-thick aluminum slab. The contrast is measured by rotating a phase-shifting "flag" of thickness T (see Fig. 2) through small angles about an axis perpendicular to the plane of the interferometer. It is easy to show that the phase shift corresponding to a given small rotation angle δ is

$$\varphi_{\text{flag}} = -2\lambda N' b' T \delta \sin\theta_B / \cos^2\theta_B, \quad (7)$$

and the counting rate in the ^3He detector varies as

$$I = A + B \cos(\varphi_{\text{flag}} + \varphi_{A1}). \quad (8)$$

Here φ_{A1} is the phase shift experienced by the beam due to passage through the aluminum slab, N' is the atom density and b' the scattering length appropriate to the material of the phase-shifting

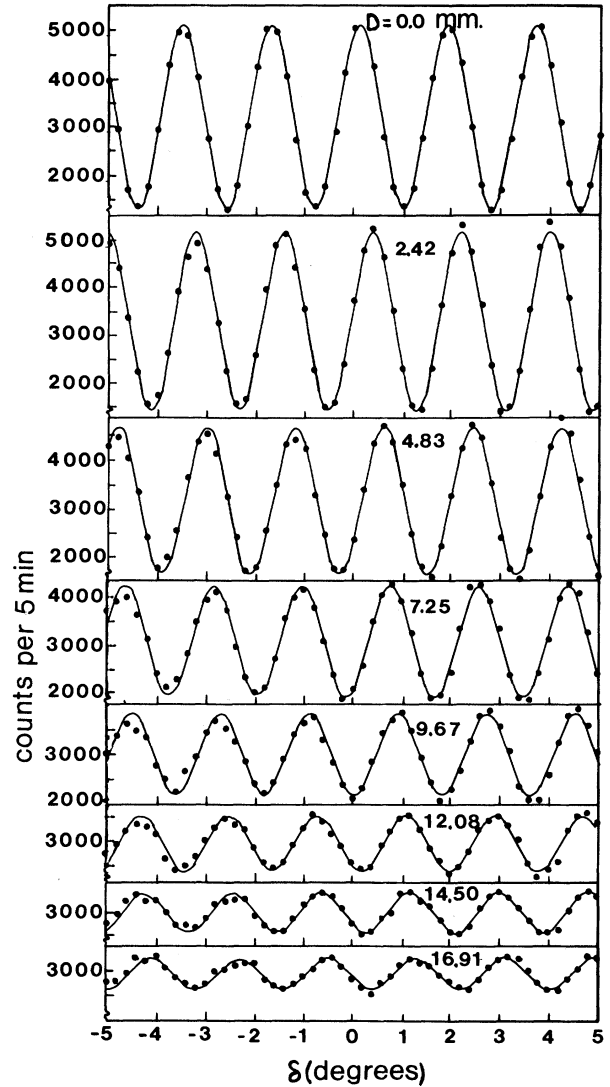


FIG. 3. Intensity oscillations observed in the interferometer resulting from rotating the phase-shifting flag through small angles, δ , as shown in Fig. 2. Each curve is for a different aluminum slab thickness, D , and therefore, a different spatial shift Δx .

flag, and θ_B is the interferometer Bragg angle. Figure 3 shows a series of interference oscillations obtained in this way, for various aluminum slabs of thickness D placed in beam II between points A and C. It is observed that there is a substantial and continuous loss of contrast as the thickness D increases.⁹ A similar set of data was taken with the aluminum slabs placed in beam path I between A and B. The contrast $[=(I_{\text{max}} - I_{\text{min}})/(I_{\text{max}} + I_{\text{min}})]$ as a function of D is displayed in Fig. 4 (curve A). The inherent contrast of the interferometer (at $D = 0$) is not 100%. This is due

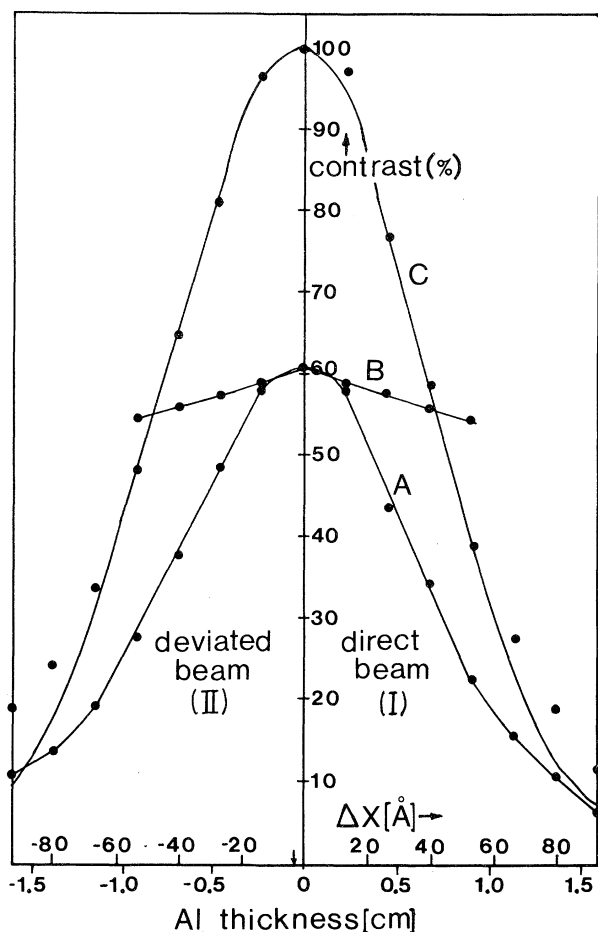


FIG. 4. Curve A: Loss of contrast as a function of aluminum slab thickness D . The abscissa is also labeled in terms of the spatial shift Δx [Eq. (6)] of the wave packet traversing the aluminum slabs. Curve B: Change of contrast vs D when identical aluminum slabs are placed in both beams. Curve C: Loss of contrast, corrected for aluminum slab inhomogeneities, thickness variations, and wave amplitude attenuation, and normalized to 100% at the peak, as discussed in the text.

to the fact that the beam splitters and the distances between the crystal plates are not perfect and precise.

From what has been said above, it is natural to interpret this loss of contrast as being due to the relative spatial shift of the wave packet in one leg of the interferometer with respect to the wave packet in the other leg caused by the delay that it experiences in passing through a progressively longer region of positive potential. However, variations in density or thickness of the aluminum slabs over the cross-sectional area of the beam and attenuation of the wave amplitude in one leg

of the interferometer due to absorption and scattering by the aluminum slabs can also cause a loss of contrast. The first of these effects can be assessed by placing aluminum slabs of identical thicknesses in both beams and observing the loss of contrast. Results of measurements of this type are shown by curve B in Fig. 4. The attenuation of the wave amplitude was found to be about 10% for 1 cm of aluminum. It was measured directly in the interferometer by blocking off the other beam with a Cd absorber. The loss of contrast due to the combination of these two effects is small, of order 5% for 1 cm of aluminum. Correcting the results for these effects, the contrast normalized to 100% at the peak is shown as curve C in Fig. 4. The solid curve, passing through most of the data points, is a Gaussian with full width at half maximum equal to 94 Å. It is centered at $\Delta x = -4$ Å, reflecting the fact that the two beam paths are not precisely equal.

In principle, the change of contrast as a function of the relative spatial shift Δx (after correction for the above two small effects) is the convolution of the wave packet $\psi_I(x, t)$ with the wave packet $\psi_{II}(x, t)$ integrated over the detector and averaged over time. Naively, one might expect the width of this curve to be the root mean square of the widths of the two packets; but, at what time? If we start the clock at the time when the neutron enters the interferometer and is Bragg reflected at the first crystal and use the transit time ($\approx 25 \mu\text{sec}$) from point A to point D and the measured wavelength spread ($\Delta\lambda/\lambda \approx 0.0125$) of the neutrons Bragg reflected by the interferometer crystals to calculate σ_k ($\approx 0.0254 \text{ \AA}^{-1}$), we find that the time-dependent contribution to the width given by Eq. (3) is about $5 \times 10^6 \text{ \AA}$, which is much larger than the 94 Å full width at half maximum observed for the experimental convolution of the two wave packets. The 94 Å width corresponds to the convolution of two packets, each of width $94/\sqrt{2} \text{ \AA}$. This implies that the equivalent Gaussian width parameter of ψ_I or ψ_{II} is 28.2 Å; the Gaussian width of the probability densities ($|\psi_I|^2$ or $|\psi_{II}|^2$) is then $\sigma_x = 19.9 \text{ \AA}$. This means that $\sigma_x \sigma_k \approx 0.505$, which is consistent with Eq. (1), implying that this experiment directly measures the minimal width $\sigma_x(0)$.

The fact that the spreading of the wave packet with time does not seem to play a role in these observations can be understood theoretically. If one looks in detail at the internal structure of, say, a Gaussian packet, it is found that $\psi(x, t)$ is not symmetric about its center; the wavelength

of the oscillations in real space is somewhat longer on the trailing edge than on the leading edge. Therefore, interference effects are only observable when the two wave packets are nearly coincident as discussed by Klein, Opat, and Hamilton.¹⁰ To our knowledge, this is the first experiment in which the detailed longitudinal shape of a neutron wave packet has been observed, and the uncertainty relation for neutrons in the longitudinal direction explicitly verified.

One of us (S.A.W.) would like to acknowledge useful discussions with A. G. Klein (Melbourne) and H. Rauch (Vienna). This work was supported by the National Science Foundation under Grant No. PHY-7920979.

^(a)Visiting summer student from Physics Department, University of Arizona, Tucson, Ariz. 85720.

¹L. I. Schiff, *Quantum Mechanics* (McGraw-Hill, New York, 1955 2nd. ed., pp. 54-59.

²G. Möllenstedt and G. Wohland, in *Electron Microscopy 1980*, edited by P. Bredoro and G. Boom (Seventh European Congress on Electron Microscopy Foundation, Leiden, 1980), Vol. 1, p. 28.

³U. Bonse and M. Hart, *Appl. Phys. Lett.* **6**, 155 (1965).

⁴H. Rauch, W. Treimer, and U. Bonse, *Phys. Lett.* **47A**, 425 (1974).

⁵See *Neutron Interferometry, Proceedings of an International Workshop*, edited by U. Bonse and H. Rauch (Clarendon, Oxford, 1979).

⁶S. A. Werner, *Phys. Today* **33**, 24 (1980).

⁷A. G. Klein and S. A. Werner, *Rep. Prog. Phys.* (to be published).

⁸V. F. Sears, *Phys. Rep.* **82**, 1 (1982).

⁹H. Rauch, in *Neutron Interferometry, Proceedings of an International Workshop*, edited by U. Bonse and H. Rauch (Clarendon, Oxford, 1979), pp. 161-194. This review paper describes an experiment carried out at the Institute Laue-Langevin in Grenoble in which loss of contrast at very high orders of interference was observed.

¹⁰A. G. Klein, G. I. Opat, and W. A. Hamilton, following Letter [*Phys. Rev. Lett.* **50**, 563 (1983)].

Longitudinal Coherence in Neutron Interferometry

A. G. Klein, G. I. Opat, and W. A. Hamilton

School of Physics, University of Melbourne, Parkville, Victoria 3052, Australia

(Received 27 December 1982)

The proposition that the coherence length of de Broglie wave packets remains unchanged even though the length of the packets increases upon propagation is discussed and demonstrated.

PACS numbers: 03.65.Bz, 42.50.+q

An interesting conceptual difference between classical interferometry and neutron interferometry is brought into evidence by the experiment of Kaiser, Werner, and George.¹ It concerns the question of longitudinal coherence and is due to the intrinsically dispersive propagation of massive de Broglie waves. The problem may be illustrated with reference to a Gaussian wave packet propagating in accord with the Schrödinger equation. The width of the packet, as shown in Fig. 1, increases according to the expression²

$$\sigma_x^2(t) = \sigma_x^2(0) + [\hbar t/2m\sigma_x(0)]^2. \quad (1)$$

Neutrons, which may be represented by such a wave packet, are coherently split in a neutron interferometer and are later recombined after traveling along unequal optical paths. It is obvious that no interference is to be observed if the

path difference, Δx , exceeds the spatial extent of the wave packet. However, if the interferometer is a long way downstream from the monochromator (in which the initial packet was prepared), the partial packets will now overlap, as shown in Fig. 2. May we now expect an observable interference pattern?

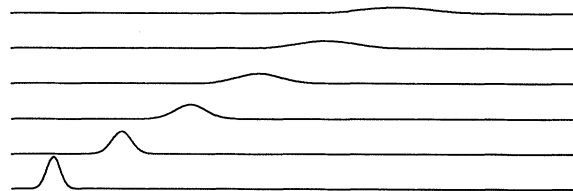


FIG. 1. Evolution of a freely propagating Gaussian wave packet.